Optical study of electronic structures and phonons in alkali-metal-doped C_{60}

Y. Iwasa

Japan Advanced Institute of Science and Technology, Ishikawa 923-12, Japan

T. Kaneyasu*

Department of Applied Physics, The University of Tokyo, Tokyo 113, Japan
(Received 1 September 1994)

We have measured optical reflection spectra for the alkali-metal fullerides K_3C_{60}, Rb_3C_{60}, K_4C_{60}, Rb_4C_{60}, and Rb_6C_{60} grown by a cosublimation method in an energy region of 0.08–6 eV. A gap structure peaked at 0.5 eV was observed in K_4C_{60}, indicating that this compound is an insulator. This result is in good agreement with other kinds of experiments, but contrary to a simple band theory. The metallic conductivity spectra of K_3C_{60} and Rb_3C_{60} were formed of a Drude part and midinfrared absorption. The energy of the latter contribution was close to the optical gap of K_4C_{60}. The infrared-active molecular vibrational $T_{1u}(4)$ mode shows an anomalous dependence on the alkali concentration x, and a large splitting (about 30 cm^{-1}) in the $x=4$ phase. These results suggest that the interaction between the doped electrons and the $T_{1u}(4)$ vibration mode is extremely strong. The relation between the anomalous phonons and the midinfrared absorption in K_4C_{60} and K_3C_{60} is discussed.

I. INTRODUCTION

The electronic structures of alkali-metal (A) fullerides (A_xC_{60}) have been a subject of considerable interest because high T_c superconductivity has been discovered in this class of materials.[1] A number of theoretical and experimental studies have been made on these materials to clarify the electronic structures. For the superconducting A_3C_{60}(A =K and Rb), a Fermi liquid theory seems to work.[2] A simple band calculation explains the electronic properties qualitatively, but not quantitatively. In several experiments, an enhancement of the density of states $N(\epsilon_F)$ at the Fermi energy ϵ_F is observed.[3,4] For instance, Ramirez et al. reported that the magnetic susceptibility [$\propto N(\epsilon_F)$] is enhanced by the factor of 1.4–2.3 comparing to the band model, and suggested the possibility of Stoner enhancement.[3] On the other hand, Degiorgi et al.[5] measured the far-infrared (ir) reflectivity and claimed that the true plasma edge exists at significantly lower energy than the value predicted by the band theory.[6] However, the relation between the $N(\epsilon_F)$ enhancement at zero frequency and the high frequency electrodynamic response remains an open question.

In contrast to the superconducting A_3C_{60} compounds, the nature of the nonsuperconducting compounds AC_{60}, A_2C_{60}, and A_4C_{60}(A =K, Rb, or Cs) is poorly understood. Band theories predict that all these compounds are metallic.[7,8] However, most of the experimental results suggest that A_4C_{60} is insulating.[9–12] As for AC_{60}, it is reported that the low temperature electronic state depends on the cooling rate: Quenched samples behave like an insulator, while annealed ones are metallic above 50 K.[13,14] Among these, the absence of metallic behavior in the $x=4$ system is particularly important, since the failure of the simple band theory is experimentally established. This subject is also important in the context of the proximity of superconductivity and insu-

lating phases. The microscopic mechanism of the insulating state is not understood yet.

In this paper we report optical spectra for K_3C_{60}, Rb_3C_{60}, K_4C_{60}, and Rb_4C_{60} to clarify the low energy excitation and phonons in these compounds. Spectra for the undoped C_{60} and fully doped Rb_6C_{60} are shown in comparison. Although a large amount of work has been done on the optical properties of doped C_{60},[15–18,5,19–21] most of these works were done on thin film samples. Instead, our sample for the optical measurement has been grown by a cosublimation method,[18] in which both alkali metal and C_{60} are simultaneously vaporized. The advantage of this method over *in situ* measurements on thin films is that the samples can be characterized by both x-ray diffraction and Raman spectra.

We found that the optical conductivity spectra of C_{60} and Rb_6C_{60} are characteristic of insulators, in accord with other experiments and band calculations. However, for K_4C_{60}, we observe insulating behavior with the lowest conductivity peak at about 0.5 eV. This is in contradiction to the band theory, but in agreement with other experiments, such as photoemission,[22,23] NMR,[10] muon-spin resonance (μSR),[11] and spin susceptibilities.[12] The plasma energy ω_P was derived by a spectral analysis for K_3C_{60} and Rb_3C_{60}. To explain the precise features of the conductivity spectra, a simple Drude model is not sufficient, but we must assume a Lorentz oscillator centered at 0.4–0.5 eV in addition to the Drude part.

We also investigated the molecular vibration modes. We determined the x dependence of the wave number, linewidth, and intensities of the infrared-active $T_{1u}(4)$ mode. This mode shows an anomalous softening upon doping and is split into two in A_4C_{60}.

II. EXPERIMENT

The A_xC_{60} samples described in this study were grown by a cosublimation technique in a temperature-gradient

furnace.[18] An evacuated quartz tube is placed in a furnace having two temperature zones, a hot end (550–590 °C) for the sublimation of C_{60} and a cooler end (200–450 °C) for the vaporization of alkali metals. The growth conditions of K_3C_{60} and K_4C_{60} differ from each other. For K_3C_{60}, the hot and cold ends were kept at 570 °C and 350 °C, respectively. In the case of K_4C_{60}, the temperatures at both ends were a few tens of degrees higher than those for K_3C_{60}. Rb compounds were grown by the same method. The temperature at the cold end was about 200 °C, and the hot end was about 550 °C for Rb_3C_{60}. Higher temperatures were also necessary for the growth of Rb_4C_{60} and Rb_6C_{60}. After a few days of reaction, flakelike samples were formed in the middle part of the tube. The $x = 4$ phase samples (K_4C_{60} and Rb_4C_{60}) were usually obtained as a mixture with $x = 6$ phases. A deintercalation process was necessary to get pure samples of A_4C_{60}.

The sample surfaces were slightly round since they are a trace of the inner wall of the quartz tube. Therefore an optical microscope was used for the measurement of the optical reflection spectra. On the scale of the microscope, the sample surfaces were flat and shiny, showing sufficient optical qualities.

For characterization of the cosublimated samples, we measured x-ray diffraction patterns. The x-ray data confirmed that the obtained samples were polycrystalline but in a single phase. A contamination of impurity phases was several percent at most, which does not seriously affect the quality of the optical reflection data. For another characterization, Raman spectra of the pentagonal pinch $A_g(2)$ mode were measured. Figure 1 shows the Raman spectra around the $A_g(2)$ mode for pristine C_{60}, K_3C_{60}, Rb_4C_{60}, and Rb_6C_{60}. In contrast to the x-ray measurements, the Raman spectra probes the surface on the scale of the penetration depth of light. Accordingly, the Raman measurement is an important characterization of the samples for reflection measurements. The single peak feature is further evidence for the absence of phase separation on the surface of cosublimated samples. The $A_g(2)$ mode has been known as a useful probe for the molecular valence of C_{60}. Since this mode is known to shift almost linearly with the alkali-metal concentration x (see Fig. 9), we can determine the x value from the wave number of this mode. (The Raman shift of the $A_g(2)$ mode in Rb_6C_{60} is slightly smaller than the reported values.[24–26] The reason for the difference is not clear.)

Optical reflection measurements were made at room temperature only for the samples which were confirmed to be in a single phase by these characterizations. The samples were sealed in a hand-made vacuum cell having an appropriate optical window in order to prevent degradation by air.

III. RESULTS

A. Electronic transitions

Figure 2 shows the reflection spectra of C_{60}, K_3C_{60}, K_4C_{60}, and Rb_6C_{60}. The spectrum for C_{60} was taken for the (111) as-grown surface of single crystals. The reflectivity in the mid-ir region is small for C_{60} and Rb_6C_{60}, indicating that these materials are insulators. For K_3C_{60} and K_4C_{60}, the reflectivity at low energy is relatively high, indicating that there exist excitations in the lower energy region. The small structures in the ir region in pristine C_{60} are attributed to the intramolecular tangential vibration mode. One of the modes $[T_{1u}(4)]$ shows a drastic increase of intensity upon doping.

Figure 3 shows the optical conductivity spectra of C_{60}, K_3C_{60}, K_4C_{60}, and Rb_6C_{60}, derived by a Kramers-Kronig transformation. In the undoped C_{60}, the onset of electronic transition is observed at 1.7–1.8 eV, consistent with the reported values. In the doped materials, the spectral weight is shifted to lower energy. The spectra below 2 eV in doped C_{60} are attributable to the contribution from the introduced electrons. According to molec-
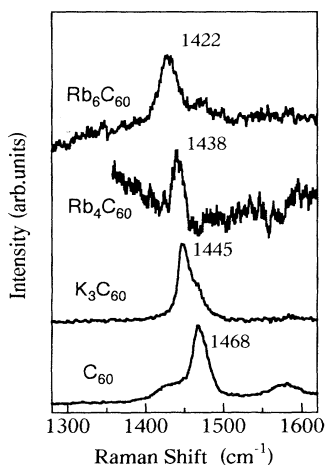

FIG. 1. Raman scattering spectra of C_{60}, K_3C_{60}, Rb_4C_{60}, and Rb_6C_{60}. The Raman shifts of the $A_g(2)$ mode are shown.
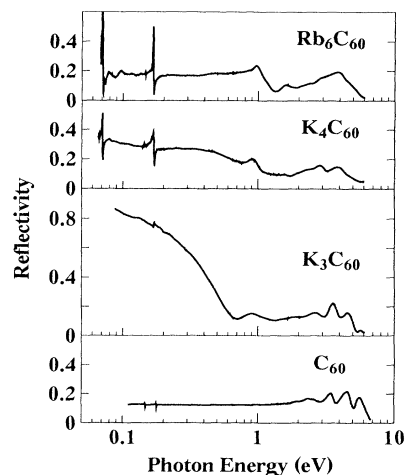

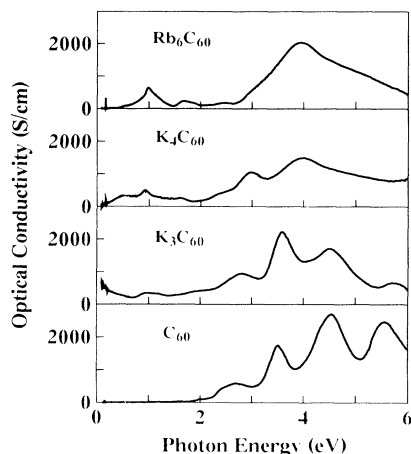FIG. 2. Reflectivity spectra of C_{60}, K_3C_{60}, K_4C_{60}, and Rb_6C_{60}.

FIG. 3. Optical conductivity spectra of C_{60}, K_3C_{60}, K_4C_4, and Rb_6C_{60}.

ular orbital calculations,[27,28] the excitations below and above 0.7 eV are ascribed to the inter- and intra-molecular transitions, respectively.

The spectrum of K_3C_{60} is sharp, compared to the previous reports. Considering the similar spectral shape of C_{60} and K_3C_{60}, our tentative interpretation is that each peak is shifted to lower energy by about 1 eV in K_3C_{60}. This trend is qualitatively, but not quantitatively, in accord with the electron energy loss spectra (EELS) by Sohmen and Fink[29] and theoretical calculation.[30] In K_4C_{60}, a broadening of the spectra above 2 eV makes peak assignment difficult. In Rb_6C_{60}, only a weak structure is observed near 2.5 eV, where a strong peak was found both in the absorption[17] and the EELS.[29] The reason for the disagreement is not clear. The surface quality might affect the reflection spectra in the high energy region.

Figure 4 shows the conductivity spectra in the lower energy region. In the doped materials, a peak near 1 eV
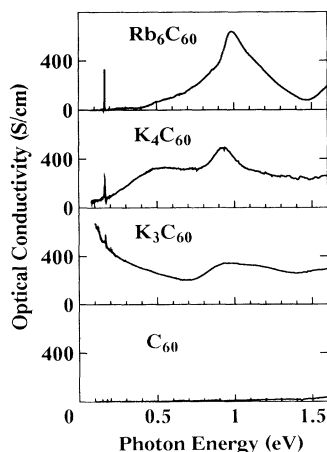
is commonly observed. According to the calculation of molecular orbital and band structure of C_{60}, this peak is assigned to the transition from the lowest unoccupied molecular orbital (LUMO) (t_{1u}) to the next LUMO (t_{1g}). In addition to the 1 eV transition, we observe a Drude-like conductivity spectrum in K_3C_{60}. Detailed features of the spectrum are discussed later in comparison with the spectra of Rb_3C_{60} and K_4C_{60}.

In contrast to the metallic features of K_3C_{60}, the conductivity of K_4C_{60} at low energy decreases with the photon energy, indicating that K_4C_{60} is an insulator. The lowest absorption peak is located at around 0.5 eV. This behavior is not understood in the framework of the simple band picture, which predicts that the $x = 4$ compound is metallic since the triply degenerate t_{1u} LUMO is still partially filled. In fact, the band calculation[7] shows that the metallic state is maintained in K_4C_{60} although the symmetry of the bct structure is low in comparison with the fcc structure.

When we compare the present result with other experimental results, on the other hands, we find fairly good agreement. The μSR measurements found that both K_4C_{60} and K_6C_{60} are insulators. It is interesting to point out that the energy gap (~ 0.3 eV) of K_4C_{60} estimated from the temperature dependence of the relaxation time T_2 of μSR (Ref. 11) is close to the lowest peak energy in the optical conductivity spectra. The T_1 of NMR displays a non-Korringa-like behavior in Rb_4C_{60}, supporting an insulating state of the $x = 4$ phase.[10] A Curie-like spin susceptibility[12] and photoemission spectra[22,23] also confirm the insulating state of K_4C_{60}.

In Rb_6C_{60}, the mid-ir region becomes silent again, because the t_{1u} band is fully occupied by the electrons transferred from the alkali metal. The lowest electronic excitation is the $t_{1u} \rightarrow t_{1g}$ interband (intramolecular) transition. These features are in reasonable agreement with the previous results.[15]

Figure 5 shows the conductivity spectra of K_3C_{60} and Rb_3C_{60}. Drude-like excitation at low energy and the lowest intraband transition around 1 eV are commonly observed in both compounds, indicating that these compounds have similar electronic structures. As shown
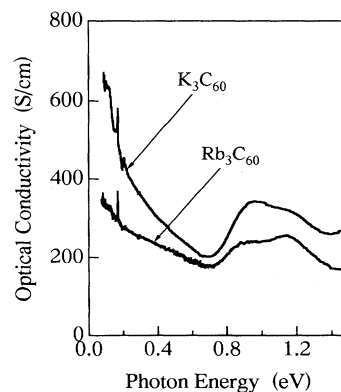

FIG. 4. Infrared conductivity spectra of C_{60}, K_3C_{60}, K_4C_{60}, and Rb_6C_{60}.

FIG. 5. Infrared conductivity spectra of K_3C_{60} and Rb_3C_{60}.

above, the peak at 1 eV is the lowest intramolecular excitation, and the excitation below 0.7 eV is ascribed to the intermolecular transition.

Apparently, the spectral weight below 0.7 eV is smaller in K_3C_{60} than that in K_3C_{60}. This trend qualitatively agrees with the band picture, which predicts a smaller bandwidth (larger effective mass) in Rb_3C_{60}. It is also obvious that both spectra deviate from a simple Drude model. As we showed in previous reports, a single Drude excitation can roughly fit the mid-ir data,[18] but not completely. Here we assume that the spectrum below 0.7 eV is composed of a single Drude excitation and a Lorentz oscillator centered at around 0.5 eV. In view of these features we model the dielectric function with the following expression:

$$\epsilon(\omega) = \epsilon_\infty + \omega_P^2 \left\{ -\frac{f_d}{\omega(\omega + i\gamma_P)} + \frac{1 - f_d}{\omega_1^2 - \omega^2 - i\omega\gamma_1} \right\}$$
$$+ \frac{\omega_L^2}{\omega_2^2 - \omega^2 - i\omega\gamma_2} . \tag{1}$$

ϵ_∞ is the high frequency dielectric constant. The second term is the mid-ir excitation, and the last term corresponds to the 1 eV interband transition. The second term is divided into Drude and Lorentz parts. Here, the expression of the second term is exactly the same as that used in Ref. 5, but the energy of the Lorentz part is different. The third term is the lowest intramolecular excitation ($t_{1u} \rightarrow t_{1g}$) at about 1 eV.

The best fit curves are shown in Fig. 6 for K_3C_{60}, Rb_3C_{60}, and K_4C_{60} by thin solid lines. In the case of K_4C_{60}, we assume that the Drude component is zero, considering the insulating nature of this compound. A fair agreement is obtained in the range of $0.08 \leq \hbar\omega \leq 1$ eV for these materials. The parameters used in the fit in Fig. 6 are tabulated in Table I. To obtain a satisfactory fit to the mid-ir spectra of K_3C_{60} and Rb_3C_{60}, a Lorentz oscillator centered at 0.4–0.5 eV was necessary. In other words, the simple Drude model does not work in the mid-ir region. Note that the energy of the Lorentz part is similar to the gap in K_4C_{60}. This band is not ascribed to an effect of contamination of the $x=4$ compounds, because the amount of impurity phases is estimated to be negligibly small from the Raman and x-ray data. There-

TABLE I. Parameters derived from the fit of the conductivity spectra in Fig. 6 using Eq. (1).

	ω_P (eV)	γ_P (eV)	f_d	ω_1 (eV)	γ_1 (eV)	ω_L (eV)	ω_2 (eV)	γ_2 (eV)
K_3C_{60}	1.34	0.18	0.65	0.42	0.56	0.82	0.96	0.34
Rb_3C_{60}	1.14	0.30	0.61	0.48	0.62	0.60	0.91	0.31
K_4C_{60}	1.34		1	0.54	0.77	0.73	0.95	0.24

fore, we conclude that the mid-ir Lorentz part (absorption) in K_3C_{60} and Rb_3C_{60} is intrinsic.

The parameters for the Drude parts should be checked by dc-resistivity measurement. According to the recent experiment on crystalline films by Palstra et al.,[2] the room temperature conductivity is 800 and 360 S/cm for K_3C_{60} and Rb_3C_{60}, respectively. The parameters in Table I, on the other hand, give the dc conductivity of 870 and 355 S/cm, in good agreement with Palstra's data. This result supports the appropriateness of the fit in Fig. 6.

The plasma energy of the Drude term $\sqrt{f_d}\omega_P$ in Eq. (1) is estimated at 1.08 and 0.89 eV for K_3C_{60} and Rb_3C_{60}, respectively. Erwin and Pickett[6] derived the plasma energy of 1.2 eV for K_3C_{60}. The ratio of the plasma energy for K_3C_{60} and Rb_3C_{60} is 1.21. In the free electron model, the plasma energy is proportional to $\sqrt{n/m^*}$ (n is the carrier density, and m^* is the effective mass). Since n is almost the same for the two compounds, it is concluded that the effective mass ratio is 0.69. This value is in accord with the band calculation.[31] [The plasma energy of K_3C_{60} obtained in the present work is considerably smaller than the value (1.5 eV) determined by our previous paper.[18] This is because the mid-ir data were analyzed in terms of a single Drude excitation in the previous work, and the 0.5 eV Lorentz part was included in the plasma energy.]

Degiorgi et al.[5] measured the reflection spectra for single crystals and polycrystals of K_3C_{60} and Rb_3C_{60}. They estimated the ω_P value at 1.17 and 1.14 eV for K_3C_{60} and Rb_3C_{60}, respectively. These values correspond to $\sqrt{f_d}\omega_P$ in our analysis. While the agreement between the present results and Ref. 5 is good in K_3C_{60}, it is not in
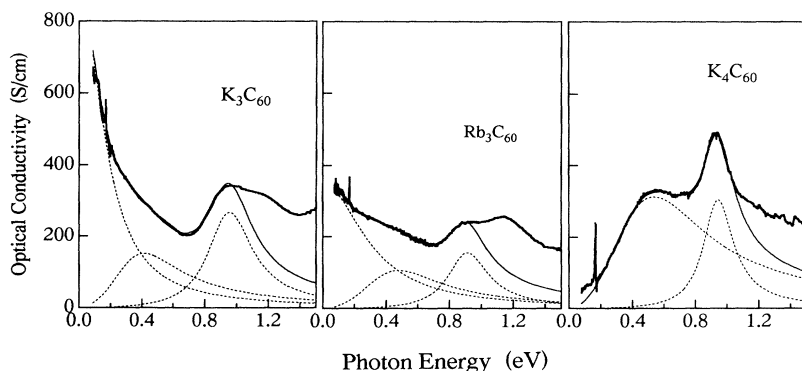

FIG. 6. Conductivity spectra of K_3C_{60}, Rb_3C_{60}, and K_4C_{60}. The best fit curves based on Eq. (1) are shown by thin solid lines. Contributions from the Drude and two Lorentz parts are shown by thin broken lines. The parameters are summarized in Table. I.

Rb_3C_{60}. In Ref. 5 the plasma energies of K_3C_{60} and Rb_3C_{60} are almost the same, in contrast to our results and the band calculation. They also found a conductivity peak at 0.05 eV, and showed that the mid-ir spectra which we are discussing are the tail of a large Lorentzian oscillator. The far-ir data by Degiorgi et al.[5] may suggest some mechanism of renormalization of ω_P.

In this subsection, we showed the optical conductivity of alkali-metal-doped C_{60} compounds, and found an optical gap in K_4C_{60}. We also showed that the conductivity spectra of K_3C_{60} and Rb_3C_{60} in the 0.08–0.7 eV region are composed of Drude and mid-ir absorptions.

B. Phonons

Figure 7 shows conductivity spectra of the ir-active intramolecular vibration modes for C_{60}, K_3C_{60}, K_4C_{60}, and Rb_6C_{60}. The peaks at 1182 and 1428 cm^{-1} for C_{60} are assigned to the $T_{1u}(3)$ and $T_{1u}(4)$ modes, respectively. These modes are tangential vibrations of C_{60} skeletons. A drastic increase in peak intensity and decrease in wave number are observed in the $T_{1u}(4)$ mode. In contrast, the $T_{1u}(3)$ mode does not show a remarkable change between C_{60} and Rb_6C_{60}, although we did not observe any well-defined peak of $T_{1u}(3)$ in the $x=3$ and $x=4$ phases. These results indicate that $T_{1u}(4)$, having more double-bond-like character, has an extraordinarily strong coupling constant with the electrons introduced in the t_{1u} conduction band.

In the spectrum of K_4C_{60}, we see a clear splitting of 30 cm^{-1} in the $T_{1u}(4)$ mode. The peak of the lower component is at 1320 cm^{-1} lower than that for Rb_6C_{60}. This is a strong indication that the lower component observed in K_4C_{60} is not attributable to extrinsic effects such as phase separation in the sample, but is intrinsic in origin. The splitting was not found in the $T_{1u}(2)$ mode. Similar results were recently found by Pichler et al.[21]

For more precise discussion, we made a spectral shape analysis on the $T_{1u}(4)$ mode assuming a Lorentzian line shape
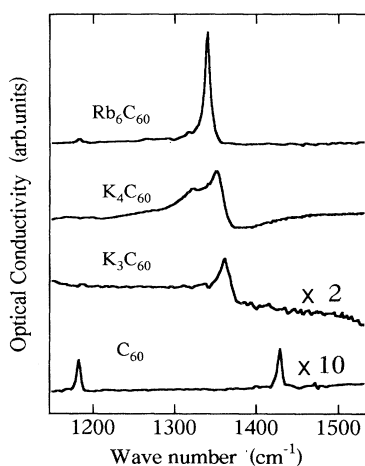
$$\epsilon(\omega)=\epsilon_b(\omega)+\frac{\omega_{L1}^2}{\omega_{t1}^2-\omega^2-i\omega\gamma_{t1}}+\frac{\omega_{L2}^2}{\omega_{t2}^2-\omega^2-i\omega\gamma_{t2}} \ . \quad (2)$$

Here, the broad background electronic contribution $\epsilon_b(\omega)$ is approximated by a smooth function in the vicinity of the $T_{1u}(4)$ phonon. The third term was zero ($\omega_{L2}=0$) except for A_4C_{60}. The best fit curves are shown by thin lines in Fig. 8 for A_3C_{60} and A_4C_{60} ($A=K$ and Rb), and the parameters are summarized in Table II. From these data, we conclude that the phonon spectra do not depend strongly on the alkali metal. A small difference is seen in the width and intensity ratio of split bands in $x=4$ compounds.

The wave numbers ω_{t1} and ω_{t2} of the $T_{1u}(4)$ mode are plotted against the alkali-metal concentration x in the left panel of Fig. 9. The x dependence of the Raman-active $A_g(2)$ mode is also plotted for comparison. Although both of these modes originate from the C=C stretching motion, the symmetry is different. In sharp contrast to the $A_g(2)$ mode which shifts almost linearly against x, the $T_{1u}(4)$ mode shows a strong downward bending. This result suggests that there exists an anomalous electron-molecular vibration (EMV) coupling in this mode. Another interesting feature is, as was pointed out earlier, the splitting of 30 cm^{-1} in both K_4C_{60} and Rb_4C_{60}.

The right panel of Fig. 9 shows the x dependence of the linewidths γ_{t1} and γ_{t2}. This parameter goes through a maximum at $x=4$. We can attribute this broadening to an intrinsic property. First, the reproducibility of the peak width was good for both K_4C_{60} and Rb_4C_{60}. Second, the possibility of poor crystallinity is excluded, since the x-ray diffraction peak width is as small as that of $x=3$ and 6 compounds (only slightly larger than the experimental resolution). This result indicates that there exists an unknown mechanism which broadens the $T_{1u}(4)$ mode except for a conduction-electron–phonon interaction. The nonlinear shift in wave number and the large width in A_4C_{60} suggest that the Rice and Choi
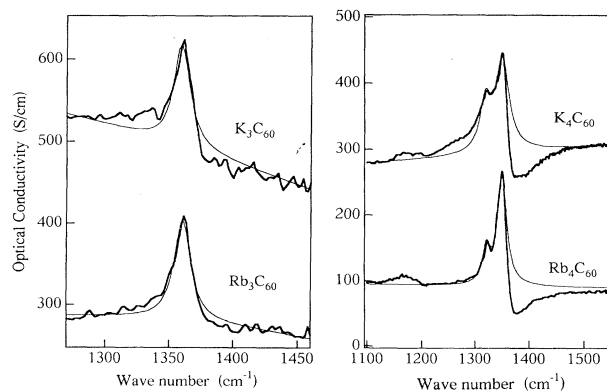

FIG. 7. Optical conductivity spectra of phonons for C_{60}, K_3C_{60}, K_4C_{60}, and Rb_6C_{60}.

FIG. 8. $T_{1u}(4)$ phonon spectra of K_3C_{60} and Rb_3C_{60} (left panel) and K_4C_{60} and Rb_6C_{60} (right panel). The fitted curves based on Eq. (2) are shown as thin solid lines. The spectrum of K_4C_{60} is shifted upwards. The parameters are summarized in Table II.
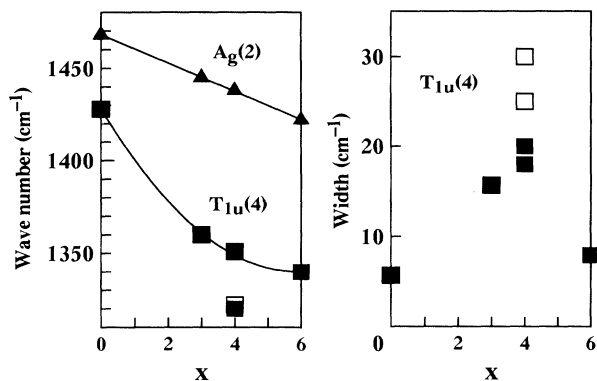
FIG. 9. Wave numbers ω_{t1},ω_{t2} (left panel) and linewidths γ_{t1},γ_{t2} (right panel) of $T_{1u}(4)$ mode against the alkali-metal concentration x. The full and open squares are K_xC_{60} and Rb_xC_{60}, respectively. In A_4C_{60}, two plots are shown representing the splitting of the mode. In the left panel, the wave number of the $A_g(2)$ mode is plotted as triangles for reference.

theory[32] should be improved for a full understanding.

As shown in Table II, the intensity of the $T_{1u}(4)$ mode is about 40 times larger than that of pristine C_{60}. This trend is consistent with the previous reports.[15,17,19,21] This phenomenon is explained by Rice and Choi,[32] who assumed that the oscillator strength is borrowed from the intramolecular electron excitation $(t_{1u} \rightarrow t_{1g})$.

IV. DISCUSSION

A. A_4C_{60}

In the previous section, we have shown the spectrum of K_4C_{60}, in which the conductivity decreases with photon energy below 0.4 eV, indicating that this compound is an insulator. To explain the insulating state of A_4C_{60}, several mechanisms have been proposed.

(1) There may be electron localization due to the strong electron correlation.

(2) There is the possibility of charge density wave (CDW) formation along the c axis of the bct structure.

(3) The orientational disorder may result in the localization of electrons.

TABLE II. Parameters obtained from the spectral analysis in Fig. 8 using Eq. (2). All values are expressed in units of cm^{-1}.

$T_{1u}(4)$	ω_{L1}	ω_{t1}	γ_{t1}	ω_{L2}	ω_{t2}	γ_{t2}
C_{60}	23.3	1428	5.7	0		
$K_3 C_{60}$	85.7	1360	15.7	0		
Rb_3C_{60}	85.7	1360	15.7	0		
K_4C_{60}	176	1351	30	118	1320	25
Rb_4C_{60}	160	1351	20	86	1322	18
Rb_6C_{60}	146	1340	7.95	0		

(4) Jahn-Teller distortion may cause the triply degenerate LUMO to split into two.

While the model (1) predicts a magnetic ground state, the other three mechanisms result in nonmagnetic ground states. Magnetic measurements are good tests for these models. Electron spin resonance measurements show that only a Curie-like spin susceptibility is observed with a small spin density (on the order of 1/10 per C_{60}).[12] Other experiments such as NMR and μSR failed to find any magnetic ordering above 4 K. Therefore, the observed Curie-like susceptibility is possibly attributable to localized spins due to the nonstoichiometry of alkali metals, indicating that the ground state of K_4C_{60} is a nonmagnetic insulator. Thus it seems unlikely that only the strong correlation effect can explain the insulating state of A_4C_{60}.

The model (2) predicts a period doubling along the c axis,[7] which has never been observed.[33] As to the model (3), the structure of A_4C_{60} is well explained by merohedral disorder[33] analogous to the model for A_3C_{60}, in which the metallic state is maintained. Accordingly, the orientational disorder cannot be a dominant mechanism for the gap opening in A_4C_{60}.

These considerations exclude the models (2) and (3). In this manner, there is no experimental evidence that positively supports any of the above models. But the splitting of the $T_{1u}(4)$ mode that was shown in the previous section may be a clue to resolve this puzzle. Now we discuss the model (4).

In the Jahn-Teller model, the C_{60} molecules undergo a static distortion in the intercalated compound. The distortion occurs when the electronic energy gain by degeneracy lifting overcomes the energy loss due to molecular deformation. In the case of A_4C_{60}, the t_{1u} LUMO splits into two and only the lower two levels are occupied by four electrons. This makes A_4C_{60} a nonmagnetic insulator. If C_{60} molecules undergo a static Jahn-Teller distortion in A_4C_{60}, the degeneracy of the T_{1u} phonon is lifted. The 30 cm^{-1} splitting in the $T_{1u}(4)$ mode observed in A_4C_{60} (Figs. 7 and 8) might be evidence for the Jahn-Teller distortion. The intensity ratio of the two split peaks is expected to be 2:1, which is not far from the observation (Fig. 8 and Table II).

However, there is an alternative interpretation. The crystal structure of A_4C_{60} is bct. In the tetragonal crystal field, the T_{1u} mode also splits. This type of splitting was observed in the fivefold degenerate H_g mode in the Raman spectrum of bcc Rb_6C_{60}.[26] To identify the origin of the phonon splitting, a quantitative argument is necessary.

Among the four models presented for the insulating state of A_4C_{60}, only the Jahn-Teller model (4) can explain the phonon anomaly in A_4C_{60}. However, this model is not conclusive yet. We should explore more experimental evidence for explaining the gap opening in A_4C_{60}. In the real system, the electronic gap might open by a combination of the above mechanisms. In fact, a recent theory[34] shows that the gap opens as a combined effect of the electron correlation and Jahn-Teller-type electron-phonon interaction. This theory predicts a static molecu-

lar distortion which is detectable by a careful structural study.

B. A_3C_{60}

The analysis of the spectra of A_3C_{60} shows that the spectral weight of the Drude part is only 60–65 % of the total ir weight and that the remaining part is a contribution from a Lorentz oscillator peaking at 0.4–0.5 eV. There are two possible interpretations for this mid-ir absorption in K_3C_{60} and Rb_3C_{60}.

(1) One is the intra-t_{1u}-band transition which is expected from band theory. According to the band calculations,[28,6] there are two peaks in the density of states (DOS) of the t_{1u} conduction bands with a separation of 0.2–0.3 eV. Since the Fermi energy is located between these peaks, an intraband transition is expected to appear in the mid-ir region. In real crystals, due to the orientational disorder of C_{60} molecules, the sharp peaks in the DOS are smeared out.[35] This is in accord with the structureless feature of the observed conductivity spectra below 0.7 eV.

(2) The second interpretation of the 0.5 eV absorption is a pseudogap or an incoherent band. We propose the hypothesis that the origin of the gap in K_4C_{60} is related to the pseudogap opening in A_3C_{60}, because the gap energy in K_4C_{60} is close to the mid-ir absorption peak in A_3C_{60}. In the simple Drude model, the ir conductivity is composed only of a Drude oscillator with the spectral weight of $\omega_P^2/8$. Due to an electron-phonon interaction or some other mechanism, the Drude spectral weight is reduced and the remaining weight is shifted to higher energy to form an incoherent band. If we assume that the 0.5 eV absorption is ascribed only to the pseudogap, the Drude weight is $f_d \sim 0.6$ of the total ir spectral weight. If we take the theoretical value of $\omega_P = 1.2$ eV,[6] the weight reduction is 0.8.

Since the Drude spectral weight is proportional to n/m^* in the free electron model, the weight reduction corresponds to a decrease in n or an enhancement of m^*. To distinguish these two possibilities, the zero-frequency response of free carriers is helpful. The experimentally determined $N(\epsilon_F)$, which is proportional to $n^{1/3}m^*$, is large compared to the calculated values from band theories by several authors.[3,4] For instance, Ramirez et al. reported that the magnetic susceptibility $\chi[\propto N(\epsilon_F)]$ is enhanced by a factor of 1.4–2.3 compared to the band model.[3] Therefore the enhancement of m^* is a more reasonable interpretation. If this is the case, the observed Drude weight reduction corresponds to mass enhancement by a factor of 1.4–1.2.

We cannot conclude which is the dominant contribution to the 0.5 eV absorption band. The mass enhancement by a factor of 1.4 by the mechanism (2) is the upper limit. When the contribution (1) is taken into account,

this factor is smaller. Accordingly, the mass enhancement determined from the ir spectra is smaller than the observed χ enhancement.[3,4] Other mechanisms, such as the Stoner enhancement,[3] are necessary for a quantitative understanding of the large Pauli susceptibility.

Up to now, no direct evidence has been found for the Jahn-Teller effect in A_3C_{60}. This is consistent with the above considerations, because the deviation from the band picture is not so significant and therefore the molecular distortion in A_3C_{60} is expected to be small. Even if the Jahn-Teller effect exists, it might be dynamical rather than static. This makes the experimental observation more difficult. However, it is to be noted that a pseudogaplike feature was observed also in the photoemission spectra of A_3C_{60}.[23,36] These authors observed a sharp Fermi edge accompanied by a broad band. They presented different interpretations for the broad band; an incoherent band[23] and a plasmon satellite.[36]

V. SUMMARY

Optical spectra for A_3C_{60} and A_4C_{60} (A = K and Rb) are presented in comparison with those of C_{60} and Rb_6C_{60}. Discussion was focused on the mid-ir excitation in A_3C_{60} and A_4C_{60}. We found an insulating conductivity spectra in K_4C_{60} with a lowest peak of 0.4–0.5 eV. The mid-ir conductivity in K_3C_{60} and Rb_3C_{60} is composed of a Drude part and a mid-ir absorption. Since the energy of the latter oscillator is close to that in K_4C_{60}, we proposed a hypothesis that the origins of the gap in K_4C_{60} and pseudogap in K_3C_{60} are similar to each other. The Drude spectral weight is slightly reduced (by a factor of 0.6–0.8 at most), and is shifted to the higher energy peak centered at 0.4–0.5 eV. The observed reduction of ω_P^2 corresponds to the lower limit of the enhancement of $N(\epsilon_F)$ found by Ramirez et al.

The infrared-active $T_{1u}(4)$ phonon was found to show an anomalous dependence on the alkali-metal concentration x, a fairly large splitting (30 cm^{-1}) in K_4C_{60} and Rb_4C_{60}. We proposed that this splitting is due to the Jahn-Teller distortion of C_{60} molecules which also results in the breakdown of the band picture in A_4C_{60}.

*Present address: Nippon Steel Co., Yawata Works, Kitakyushu 804, Japan.

[1]A. F. Hebard, M. J. Rosseinsky, R. C. Haddon, D. W. Murphy, S. H. Glarum, T. T. M. Palstra, A. P. Ramirez, and A.

R. Kortan, Nature **350**, 600 (1991).

[2]T. T. M. Palstra, A. F. Hebard, R. C. Haddon, and P. B. Littlewood, Phys. Rev. B **50**, 3462 (1994).

[3]A. P. Ramirez, M. J. Rosseinsky, D. W. Murphy, and R. C.

Haddon, Phys. Rev. Lett. **69**, 1687 (1992).

[4]A. Jánossy, O. Chauvet, S. Pekker, J. R. Cooper, and L. Forró, Phys. Rev. Lett. **71**, 1091 (1993).

[5]L. Degiorgi, P. Wachter, G. Grüner, S.-M. Huang, J. Wiley, and K. B. Kaner, Phys. Rev. Lett. **69**, 2984 (1992); L. Degiorgi, G. Grüner, P. Wachter, S.-M. Huang, J. Wiley, R. L. Whetten, R. B. Kaner, K. Holczer, and F. Diederich, Phys. Rev. B **46**, 11 250 (1992); L. Degiorgi, E. J. Nicol, O. Klein, G. Grüner, P. Wachter, S.-M. Huang, J. Wiley, and R. B. Kaner, *ibid.* **49**, 7012 (1994); L. Degiorgi, G. Briceno, M. S. Fuhrer, A. Zettl, and P. Wachter, Nature **369**, 541 (1994).

[6]S. C. Erwin and W. E. Pickett, Science **254**, 842 (1991).

[7]S. C. Erwin, in *Buckminsterfullerenes,* edited by W. E. Billups and M. A. Ciufolini (VCH, New York, 1992).

[8]M.-Z. Huang, Y.-N. Xu, and W. Y. Ching, J. Chem. Phys. **96**, 1648 (1992).

[9]A. F. Hebard, T. T. M. Palstra, R. C. Haddon, and R. M. Fleming, Phys. Rev. B **48**, 9945 (1993).

[10]D. W. Murphy, M. J. Rosseinsky, R. M. Fleming, R. Tycko, A. P. Ramirez, R. C. Haddon, T. Siegrist, G. Dabbagh, J. C. Tully, and R. E. Walstedt, J. Phys. Chem. Solids **53**, 1321 (1992).

[11]R. F. Kiefl, T. L. Duty, J. W. Schneider, A . MacFarlane, K. Chow, J. W. Elzey, C. Niedermayer, D. R. Noakes, C. E. Stonach, B. Hitti, and J. E. Fischer, Phys. Rev. Lett. **69**, 2005 (1992).

[12]M. Kosaka, K. Tanigaki, I. Hirosawa, Y. Shimakawa, S. Kuroshima, T. W. Ebbesen, J. Mizuki, and Y. Kubo, Chem. Phys. Lett. **203**, 429 (1993).

[13]R. Tycko, G. Dabbagh, D. W. Murphy, Q. Zhu, and J. E. Fischer, Phys. Rev. B **48**, 9097 (1993).

[14]O. Chauvet, G. Oszlànyi, L. Forro, P. W. Stevens, M. Tegze, G. Faigel, and A. Jánossy, Phys. Rev. Lett. **72**, 2721 (1994).

[15]K.-J. Fu, W. L. Karney, O. L. Chapman, S.-M. Huang, R. B. Kaner, F. Diederich, K. Holczer, and R. L. Whetten, Phys. Rev. B **46**, 1937 (1992).

[16]Y. Wang, J. M. Holden, A. M. Rao, W.-T. Lee, X. X. Bi, S. L. Ren, G. W. Lehman, G. T. Hager, and P. C. Eklund, Phys.

Rev. B **45**, 14 396 (1992).

[17]T. Pichler, M. Matus, J. Kürti, and H. Kuzmany, Solid State Commun. **81**, 859 (1992).

[18]Y. Iwasa, K. Tanaka, T. Yasuda, T. Koda, and S. Koda, Phys. Rev. Lett. **69**, 2284 (1992).

[19]M. C. Martin, D. Koller, and L. Mihaly, Phys. Rev. B **47**, 14 607 (1993).

[20]W. L. Wilson, A. F. Hebard, L. R. Narasimhan, and R. C. Haddon, Phys. Rev. B **48**, 2738 (1993).

[21]T. Pichler, M. Matus, and H. Kuzmany, Solid State Commun. **86**, 221 (1993); T. Pichler, R. Winkler, and H. Kuzmany, Phys. Rev. B **49**, 15 879 (1994).

[22]P. J. Benning, D. M. Poirier, T. R. Ohno, Y. Chen, M. B. Jost, F. Stepniak, G. H. Kroll, J. H. Weaver, J. Fure, and R. E. Smalley, Phys. Rev. B **45**, 6899 (1992).

[23]T. Morikawa and T. Takahashi, Solid State Commun. **87**, 1017 (1993).

[24]S. J. Duclos, R. C. Haddon, S. Glarum, A. F. Hebard, and K. B. Lyons, Science **254**, 1624 (1991).

[25]M. G. Mitch, S. J. Chase, and J. S. Lannin, Phys. Rev. Lett. **68**, 883 (1992).

[26]P. C. Eklund, P. Zhou, K.-A. Wong, G. Dresselhaus, and M. S. Dresselhaus, J. Phys. Chem. Solids **53**, 1391 (1992).

[27]R. C. Haddon, Chem. Phys. Lett. **125**, 459 (1986).

[28]S. Saito and A. Oshiyama, Phys. Rev. Lett. **66**, 2637 (1991).

[29]E. Sohmen and J. Fink, Phys. Rev. B **47**, 14 532 (1993).

[30]Y.-N. Xu, M.-Z. Huang, and W. Y. Ching, Phys. Rev. B **44**, 13 171 (1991).

[31]A. Oshiyama, S. Saito, N. Hamada, and Y. Miyamoto, J. Phys. Chem. Solids **53**, 1457 (1992).

[32]M. J. Rice and H.-Y. Choi, Phys. Rev. B **45**, 10 173 (1992).

[33]O. Zhou and D. E. Cox, J. Phys. Chem. Solids **53**, 1373 (1992).

[34]S. Suzuki and K. Nakao (unpublished); T. Nakamine, S. Suzuki, K. Nakao, and M. Okazaki (unpublished).

[35]M. P. Gelfand and J. P. Lu, Phys. Rev. Lett. **68**, 1050 (1992); Phys. Rev. B **46**, 4367 (1992).

[36]M. Knupfer, M. Merkel, M. S. Golden, J. Fink, O. Gunnarsson, and V. P. Antropov, Phys. Rev. B **47**, 13 944 (1993).